Mon. Not. R. Astron. Soc. **375,** 1510–1520 (2007) doi:10.1111/j.1365-2966.2006.11419.x

A kinematical approach to dark energy studies

David Rapetti,⋆ Steven W. Allen, Mustafa A. Amin and Roger D. Blandford
Kavli Institute for Particle Astrophysics and Cosmology, Stanford University, 382 Via Pueblo Mall, Stanford, CA 94305-4060, USA

Accepted 2006 December 17. Received 2006 November 29; in original form 2006 May 25

ABSTRACT

We present and employ a new kinematical approach to cosmological 'dark energy' studies. We construct models in terms of the dimensionless second and third derivatives of the scalefactor $a(t)$ with respect to cosmic time t, namely the present-day value of the deceleration parameter q_0 and the cosmic jerk parameter, $j(t)$. An elegant feature of this parametrization is that all Λ cold dark matter (ΛCDM) models have $j(t) = 1$ (constant), which facilitates simple tests for departures from the ΛCDM paradigm. Applying our model to the three best available sets of redshift-independent distance measurements, from Type Ia supernova and X-ray cluster gas mass fraction measurements, we obtain clear statistical evidence for a late-time transition from a decelerating to an accelerating phase. For a flat model with constant jerk, $j(t) = j$, we measure $q_0 = -0.81 \pm 0.14$ and $j = 2.16^{+0.81}_{-0.75}$, results that are consistent with ΛCDM at about the 1σ confidence level. A standard 'dynamical' analysis of the same data, employing the Friedmann equations and modelling the dark energy as a fluid with an equation-of-state parameter, w (constant), gives $\Omega_{\rm m} = 0.306^{+0.042}_{-0.040}$ and $w = -1.15^{+0.14}_{-0.18}$, also consistent with ΛCDM at about the 1σ level. In comparison to dynamical analyses, the kinematical approach uses a different model set and employs a minimum of prior information, being independent of any particular gravity theory. The results obtained with this new approach therefore provide important additional information and we argue that both kinematical and dynamical techniques should be employed in future dark energy studies, where possible. Our results provide further interesting support for the concordance ΛCDM paradigm.

Key words: supernovae: general – cosmological parameters – cosmology: observations – cosmology: theory – X-rays: galaxies: clusters.

1 INTRODUCTION

The field of cosmology has made unprecedented progress during the past decade. This has largely been driven by new observations, including precise measurements of the spectrum of cosmic microwave background (CMB) anisotropies (Spergel et al. 2003, 2006, and references therein), the distance–redshift relation to Type Ia supernovae (SNeIa) (Riess et al. 1998; Perlmutter et al. 1999; Knop et al. 2003; Riess et al. 2004; Astier et al. 2005), the distance–redshift relation to X-ray galaxy clusters (Allen, Schmidt & Fabian 2002; Ettori, Tozzi & Rosati 2003; Allen et al. 2004), measurements of the mean matter density and amplitude of matter fluctuations from X-ray clusters (Borgani et al. 2001; Reiprich & Böhringer 2002; Allen et al. 2003; Schuecker et al. 2003; Voevodkin & Vikhlinin 2004), measurements of the matter power spectrum from galaxy redshift surveys (Tegmark et al. 2004; Cole et al. 2005; Eisenstein et al. 2005), Lyman α forest studies (Croft et al. 2002; Viel, Weller & Haehnelt 2004; Seljak et al. 2005) and weak-lensing surveys (van Waerbeke et al. 2000; Hoekstra, Yee & Gladders 2002; Jarvis et al. 2005; Van Waerbeke, Mellier & Hoekstra 2005), and measurements of the Integrated Sachs–Wolfe effect (Fosalba, Gaztanaga & Castander 2003; Scranton et al. 2003).

These and other experiments have led to the definition of the so-called concordance Λ cold dark matter (ΛCDM) cosmology. In this model, the Universe is geometrically flat with only $\sim$4 per cent of the current mass-energy budget consisting of normal baryonic matter. Approximately 23 per cent is CDM, which interacts only weakly with normal baryonic matter but which clusters under the action of gravity. The remaining $\sim$73 per cent consists of smoothly distributed quantum vacuum energy (the cosmological constant), which pushes the Universe apart. This combination of matter and vacuum energy leads to the expectation that the Universe should undergo a late-time transition from a decelerating to an accelerating phase of expansion. Late-time acceleration of the Universe is now an observed fact (e.g. Allen et al. 2004; Riess et al. 2004; Astier et al. 2006). A transition from a decelerating phase to a late-time accelerating phase is required to explain both the late-time acceleration measurements and the observed growth of structure.

Despite the observational success of the concordance ΛCDM model, significant fine-tuning problems exist. In particular,

⋆E-mail: drapetti@slac.stanford.edu

difficulties arise in adjusting the density of the vacuum energy to be a non-zero but tiny number, when compared with the value predicted by standard theoretical calculations, and in explaining why the current matter and vacuum energy densities are so similar (the 'cosmic coincidence' problem). For these reasons, amongst others, a large number of alternative cosmological models have been proposed. These include models that introduce new energy components to the Universe – so-called 'dark energy' models, for example, scalar 'quintessence' fields (Caldwell, Dave & Steinhardt 1998; Copeland, Liddle & Wands 1998; Steinhardt, Wang & Zlatev 1999; Zlatev, Wang & Steinhardt 1999; Barreiro, Copeland & Nunes 2000), *K*-essence (Armendariz-Picon, Mukhanov & Steinhardt 2000, 2001; Chiba, Okabe & Yamaguchi 2000), tachyon fields (Bagla, Jassal & Padmanabhan 2003; Copeland et al. 2005) and Chaplygin gas models (Kamenshchik, Moschella & Pasquier 2001; Bento, Bertolami & Sen 2002). Other possibilities include modified gravity theories, motivated by, for example, the existence of extra dimensions (Dvali, Gabadadze & Porrati 2000; Deffayet, Dvali & Gabadadze 2002a; Deffayet et al. 2002b; Guo et al. 2006; Maartens & Majerotto 2006) or other modifications of General Relativity (Capozziello, Carloni & Troisi 2003; Vollick 2003; Carroll et al. 2004, 2005; Navarro & Van Acoleyen 2005; Mena, Santiago & Weller 2006; Nojiri & Odintsov 2006), which can also lead to late-time cosmic acceleration. The simplicity of the concordance ΛCDM model, however, makes it highly attractive. A central goal of modern observational cosmology is to test whether this model continues to provide an adequate description of rapidly improving data.

Most current analyses of cosmological data assume General Relativity and employ the mean matter density of the Universe, $\Omega_{\rm m}$, and the dark energy equation-of-state w as model parameters. Such analyses are often referred to as 'dynamical studies', employing as they do the Friedmann equations. Other dynamical analyses employ modified Friedmann equations for a particular gravity model. However, a purely kinematical approach is also possible that does not assume any particular gravity theory. Kinematical models provide important, complementary information when seeking to understand the origin of the observed late-time accelerated expansion.

In a pioneering study, Riess et al. (2004) measured a transition from a decelerating to accelerating phase using a simple linear parametrization of the deceleration parameter $q(z)$, where $q(z)$ is the dimensionless second derivative of the scalefactor, $a(t)$, with respect to cosmic time. Recently, Shapiro & Turner (2005), Gong & Wang (2006) and Elgaroy & Multamaki (2006) have employed a variety of other parametrizations, constructed in terms of $q(z)$, to study this transition. However, since the underlying physics of the transition are unknown, the choice of a particular parametrization for $q(z)$ is quite arbitrary. Shapiro & Turner (2005) applied a principal component analysis of $q(z)$ to the SNIa data of Riess et al. (2004) and found strong evidence for recent, changing acceleration but weak evidence for a decelerated phase in the past (i.e. weak evidence for a transition between the two phases). Elgaroy & Multamaki (2006) employed a Bayesian analysis to the Riess et al. (2004) data and the more recent Supernova Legacy Survey (SNLS) SNIa sample of Astier et al. (2006), obtaining a similar result.

In this paper, we develop an improved method for studying the kinematical history of the Universe. Instead of using parametrizations constructed in terms of $q(z)$, we follow Blandford et al. (2004) and introduce the cosmic jerk, $j(a)$, the dimensionless third derivative of the scalefactor with respect to cosmic time. (Here a is the cosmic scalefactor, with $a = 1/1 + z$.) The use of the cosmic jerk formalism provides a more natural parameter space for kinematical studies. Our results are presented in terms of current deceleration parameter q_0 and $j(a)$, where the latter can be either constant or evolving. We apply our method to the three best current kinematical data sets: the'gold' sample of SNIa measurements of Riess et al. (2004), the SNIa data from the first year of the SNLS project (Astier et al. 2006), and the X-ray galaxy cluster distance measurements of Allen et al. (in preparation). The latter data set is derived from measurements of the baryonic mass fraction in the largest relaxed galaxy clusters, which is assumed to be a standard quantity for such systems (see e.g. Allen et al. 2004, for discussion).

In General Relativity, $j(a)$ depends in a non-trivial way on both $\Omega_{\rm m}$ and $w(a)$ (Blandford et al. 2004). In general, there is no one-to-one mapping between models with constant j and models with constant w. A powerful feature of the standard dynamical approach is that all ΛCDM models have $w = -1$ which make it easy to search for departures from ΛCDM. Likewise, the use of the jerk formalism imbues the kinematical analysis with a similar important feature in that all ΛCDM models are represented by a single value of $j = 1$. The use of the jerk formalism thus enables us to constrain and explore departures from ΛCDM in the kinematical framework in an equally effective manner. Moreover, by employing both the dynamical and the kinematical approaches to the analysis of a single data set, we explore a wider set of questions than with a single approach. We note that Sahni et al. (2003) and Alam et al. (2003) also drew attention to the importance of the jerk parameter for discriminating models of dark energy and/or modified gravity. Chiba & Nakamura (1998) and Caldwell & Kamionkowski (2004) also showed its relevance for probing the spatial curvature of the Universe.

Using the three kinematical data sets mentioned above, we find clear evidence for a negative value of q_0 (current acceleration) and a positive cosmic jerk, assuming j constant. The concordance ΛCDM model provides a reasonable description of the data, using both the new kinematical and the standard dynamical approaches. We also search for more complicated deviations from ΛCDM, allowing $j(a)$ to evolve as the Universe expands, in an analogous manner to dynamical studies which allow for time-variation of the dark energy equation-of-state $w(a)$. Our analysis employs a Chebyshev polynomial expansion and a Markov Chain Monte Carlo (MCMC) approach to explore parameter spaces. We find no evidence for a time-varying jerk.

This paper is structured as follows. In Section 2, we describe our new kinematical approach. In Section 3, we describe the scheme adopted for polynomial expansions of $j(a)$. Section 4 includes details of the data analysis. The results from the application of our method to the SNIa and X-ray cluster data are presented in Section 5. Finally, our main conclusions are summarized in Section 7. Throughout this paper, we assume that the Universe is geometrically flat.

2 THE KINEMATICAL AND DYNAMICAL FRAMEWORKS FOR LATE-TIME COSMIC ACCELERATION

2.1 Previous work

The expansion rate of the Universe can be written in terms of the Hubble parameter, $H = \dot{a}/a$, where a is the scalefactor and $\dot{a}$ is its first derivative with respect to time. The current value of the Hubble parameter is the Hubble Constant, usually written as H_0. Under the action of gravity, and for negligible vacuum energy, the expansion of the Universe is expected to decelerate at late times. Contrary to this expectation, in the late 1990s, SNIa experiments (Riess et al. 1998; Perlmutter et al. 1999) provided the first direct evidence for a late-time accelerated expansion of the Universe. In particular, the

present value of the deceleration parameter, q_0, measured from the supernova data was found to be negative. In detail, the deceleration parameter q is defined as the dimensionless second derivative of the scalefactor

$$q(t) = -\frac{1}{H^2}\left(\frac{\ddot{a}}{a}\right), \tag{1}$$

and in terms of the scalefactor,

$$q(a) = -\frac{1}{H}(aH)', \tag{2}$$

where the 'dots' and 'primes' denote derivatives with respect to cosmic time and scalefactor, respectively.

The current 'concordance' cosmological model, ΛCDM, has been successful in explaining the SNIa results and all other precision cosmology measurements to date. Together with its theoretical simplicity, this makes the ΛCDM model very attractive. However, as discussed in the Introduction section, the concordance model does face significant theoretical challenges and a wide range of other possible models also provide adequate descriptions of the current data (see Copeland, Sami & Tsujikawa 2006, for an extensive review).

An excellent way to distinguish between models is to obtain precise measurements of the time-evolution of the expansion of the Universe. Given such data, a number of different analysis approaches are possible. In searching for time-evolution in the deceleration parameter, as measured by current SNIa data, Riess et al. (2004) assumed a linear parametrization of $q(z)$:

$$q(z) = q_0 + \frac{\mathrm{d}q}{\mathrm{d}z}z. \tag{3}$$

These authors measured a change in sign of the deceleration parameter, from positive to negative approaching the present day, at a redshift $z_\mathrm{t} = 0.46 \pm 0.13$. Using this parametrization for $q(z)$, the definition of the deceleration parameter given by equation (1), and integrating over the redshift, we obtain that for this model the evolution of the Hubble parameter is given in the form

$$E(z) = \frac{H(z)}{H_0} = (1+z)^{(1+q_0-q')}\mathrm{e}^{q'z}, \tag{4}$$

where $q' = \mathrm{d}q/\mathrm{d}z$.

However, since the origin of cosmic acceleration is unknown, it is important to recognize that the choice of any particular parametrized expansion for $q(z)$ is essentially arbitrary. Indeed, when (or if) a transition between decelerated and accelerated phases if inferred to occur can depend on the parametrization used. Elgaroy & Multamaki (2006) showed that using the linear parametrization described by equation (3) and fitting to the SNIa data set of Astier et al. (2006) a transition redshift $z_\mathrm{t} \sim 2.0$ is obtained which, uncomfortably, lies beyond the range of the data used.

Transitions between phases of different cosmic accelerations are more naturally described by models incorporating a cosmic 'jerk'. The jerk parameter, $j(a)$, is defined as the dimensionless third derivative of the scalefactor with respect to cosmic time (Blandford et al. 2004):

$$j(t) = \frac{1}{H^3}\left(\frac{\dddot{a}}{a}\right), \tag{5}$$

and in terms of the scalefactor

$$j(a) = \frac{(a^2H^2)''}{2H^2}, \tag{6}$$

where again the 'dots' and 'primes' denote derivatives with respect to cosmic time and scalefactor, respectively.

In such models, a transition from a decelerating phase at early times to an accelerating phase at late times occurs for all models with $q_0 < 0$ and a positive cosmic jerk. Note that a Taylor expansion of the Hubble parameter around small redshifts (Riess et al. 2004; Visser 2004) contains the present value of both the deceleration and the jerk parameters, q_0 and j_0. Such Taylor expansions are inappropriate for fitting high-redshift objects (Blandford et al. 2004; Linder 2006), such as those included in the data sets used here.

Blandford et al. (2004) described how the jerk parametrization provides a convenient, alternative method to describe models close to ΛCDM. In this parametrization, flat ΛCDM models have a constant jerk with $j(a) = 1$ (note that this neglects the effects of radiation over the redshift range of interest, which is also usually the case when modelling within the dynamic framework). Thus, any deviation from $j = 1$ measures a departure from ΛCDM, just as deviations from $w = -1$ do in more standard dynamical analyses. Importantly, in comparison to dynamical approaches, however, the kinematical approach presented here both explores a different set of models and imposes fewer assumptions. The dynamical approach has other strengths, however, and can be applied to a wider range of data (e.g. CMB and growth of structure studies), making the kinematical and dynamical approaches highly complementary.

It is interesting to note that, in principle, any particular dynamical parameter space will have its own physical limits. For instance, within the dynamical (Ω_m, w) plane, models with $w < -1$, known as 'phantom' dark energy models, violate the dominant energy condition (Carroll, Hoffman & Trodden 2003; Onemli & Woodard 2004) and present serious problems relating to the treatment of dark energy perturbations (Caldwell & Doran 2005; Hu 2005; Vikman 2005; Zhao et al. 2005) when $w(z)$ crosses the boundary $w = -1$. Current data allow models with $w < -1$ (Weller & Lewis 2003; Allen et al. 2004; Riess et al. 2004; Astier et al. 2006; Cabre et al. 2006; Spergel et al. 2006) and models in which $w(z)$ crosses the boundary $w = -1$ (Corasaniti et al. 2004; Jassal, Bagla & Padmanabhan 2005; Rapetti, Allen & Weller 2005; Seljak et al. 2005; Upadhye, Ishak & Steinhardt 2005; Zhao, Xia, Feng & Zhang 2006). However, another dynamical parameter space, coming, for example, from a different gravity theory, might not pathologically suffer from such boundaries around the models allowed for current data.

Since the (q_0, j) plane (see below) is purely kinematical, that is, no particular gravity theory is assumed, we are not forced to interpret $j = 1$, or any locus in this plane, as a barrier. Note, however, that caution is required in extending the results from the kinematical analysis beyond the range of the observed data (see for details Amin & Blandford, in preparation). For example, inappropriately extending a jerk model to very high redshifts could imply an unphysical Hubble parameter at early times, that is, these models do not have a big bang in the past.

2.2 A new kinematical framework

For our kinematical analysis, we first calculate $H(a)$, given $j(a; \mathcal{C})$, where $\mathcal{C} = (c_0, c_1, ..., c_N)$ is the selected vector of parameters used to describe the evolution of $j(a)$ (see below). Following Blandford et al. (2004), we rewrite the defining equation for the jerk parameter (6) in a more convenient form:

$$a^2V''(a) - 2j(a)V(a) = 0, \tag{7}$$

where 'prime' denotes derivative with respect to a and $V(a)$ is defined as

$$V(a) = -\frac{a^2H^2}{2H_0^2}. \tag{8}$$

We specify the two constants of integration required by equation (7) in terms of the present Hubble parameter H_0 and the present deceleration parameter q_0 as follows:

$$V(1) = -\frac{1}{2}, \qquad V'(1) = q_0, \tag{9}$$

where $a(t_0) = 1$ at the present time t_0. Here, the first condition comes from $H(1) = H_0$ and the second from

$$V'(1) = -\frac{H_0'}{H_0} - 1 = q_0. \tag{10}$$

The Hubble parameter, $H(a)$, obtained from equations (7), (8) and (9) is used to calculate the angular diameter (d_A) and luminosity (d_L) distances for a flat Friedmann–Robertson–Walker–Lemaıtre (FRWL) metric:

$$d_A(a) = a^2\, d_L(a) = \frac{c}{H_0}\, a \int_a^1 \frac{1}{a^2 E(a)}\, \mathrm{d}a, \tag{11}$$

where c is the speed of light. These theoretical distances, $d_L(a)$ and $d_A(a)$, are then used in the data analysis (see Section 4).

Our framework provides a simple and intuitive approach for kinematical studies. For models with $q_0 < 0$ (>0), the Universe is currently accelerating (decelerating). Models with $q_0 < 0$ and $j(a) = 1$ (constant) are currently accelerating and have the expansion evolving in a manner consistent with ΛCDM. Any significant departure from $j = 1$ indicates that some other mechanism is responsible for the acceleration.

2.3 Standard dynamical framework

For comparison purposes, we have also carried out a standard dynamical analysis of the data in which we employ a dark energy model with a constant dark energy equation-of-state, w. From energy conservation of the dark energy fluid and the Friedmann equation, we obtain the evolution of the Hubble parameter, $H(z) = H_0\, E(z)$,

$$E(z) = \left[\Omega_m (1+z)^3 + (1-\Omega_m)(1+z)^{3(1+w)}\right]^{1/2}, \tag{12}$$

where Ω_m is the mean matter density in units of the critical density. As with the kinematical analysis, we assume flatness and neglect the effects of radiation density. In this framework, models with a cosmological constant have $w = -1$ at all times.

3 EVOLVING JERK MODELS

Our analysis allows for the possibility that the cosmic jerk parameter, $j(a)$, may evolve with the scalefactor. We have restricted our analysis to the range of a where we have data, [$a_{min} = 0.36$, $a_{max} = 1$]. In searching for possible evolution, our approach is to adopt ΛCDM as a base model and search for progressively more complicated deviations from this. We begin by allowing a constant deviation Δj from ΛCDM ($j = 1$). For this model, it is possible to solve the jerk equation (7) analytically. Using the initial conditions listed in equation (9), we obtain

$$V(a) = -\frac{\sqrt{a}}{2}\left[\left(\frac{p-u}{2p}\right)a^p + \left(\frac{p+u}{2p}\right)a^{-p}\right], \tag{13}$$

where $p \equiv (1/2)\sqrt{(1+8j)}$ and $u \equiv 2(q_0 + 1/4)$. Note that in the (q_0, j) plane for

$$j < \begin{cases} q_0 + 2q_0^2 & q_0 < -1/4 \\ -1/8 & q_0 > -1/4 \end{cases} \tag{14}$$

there is no big bang in the past.[1] The models allowed by our combined data sets do not cross this boundary.

For the next most complicated possible deviation from ΛCDM, we have $j(a;\mathcal{C}) = j^{\Lambda CDM} + \Delta j(a;\mathcal{C})$. Here $j^{\Lambda CDM} = 1$ and $j(a;\mathcal{C})$ is the cosmic jerk for the cosmology in question. In order to meaningfully increase the number of parameters in the vector $\mathcal{C}$, we employ a framework constructed from Chebyshev polynomials. The Chebyshev polynomials form a basis set of polynomials that can be used to approximate a given function over the interval [−1, 1]. We rescale this interval to locate our function $\Delta j(a;\mathcal{C})$ in the range of scalefactor where we have data

$$a_c \equiv \frac{a - (1/2)(a_{min} + a_{max})}{(1/2)(a_{max} - a_{min})}, \tag{15}$$

where a is the scalefactor in the range of interest and a_c is Chebyshev variable. The trigonometric expression for a Chebyshev polynomial of degree n is given by

$$T_n(a_c) = \cos(n \arccos a_c). \tag{16}$$

These polynomials can also be calculated using the recurrent formula

$$T_{n+1}(a_c) = 2a_c T_n(a_c) - T_{n-1}(a_c), \qquad n \geqslant 1, \tag{17}$$

where $T_0(a_c) = 1$ and, for example, the next three orders are $T_1(a_c) = a_c$, $T_2(a_c) = 2{a_c}^2 - 1$, $T_3(a_c) = 4{a_c}^3 - 3a_c$, etc. Using a weighted combination of these components, any arbitrary function can be approximately reconstructed. The underlying deviation from ΛCDM can be expressed as

$$\Delta j(a;\mathcal{C}) \simeq \sum_{n=0}^{N} c_n T_n(a_c), \tag{18}$$

where the weighting coefficients form our vector of parameters, $\mathcal{C} = (c_0, c_1, \ldots, c_N)$. Thus, using equation (18) we produce different parametrizations for increasing N. With higher values of N, we allow for a more precise exploration of the $[q_0,\, j(a;\mathcal{C})]$ parameter space. However, it is clear that this process will be limited by the ability of the current data to distinguish between such models. In order to judge how many orders of polynomials to include, we quantify the improvements to the fits obtained from the inclusion of progressively higher orders in a variety of ways (see below). In general, we find that models with a degree of complexity beyond a constant jerk are not required by current data.

We note that approches other than expanding Δj in Chebyshev polynomials are possible, for example, one could include the dimensionless fourth derivative of the scalefactor as a model parameter. However, since ΛCDM does not make any special prediction for the value of this derivative, we prefer to use our general expansion in Δj here.

4 DATA AND ANALYSIS METHODS

4.1 Type Ia supernova data

For the analysis of SNIa data, we use both the 'gold' sample of Riess et al. (2004) and the first-year SNLS sample of Astier et al. (2006).

[1] Allowed (q_0, j) values are those for which the equation $V(a) = 0$ has no solution in the past ($a < 1$) (Amin & Blandford in preparation).

The former data set contains 157[2] SNeIa, where a subset of 37 low-redshift objects are in common with the data of Astier et al. (2005). Astier et al. (2006) contain 115[3] objects. We use the measurements of Astier et al. (2006) for objects in common between the studies. Thus, combining both data sets we have 120 SNeIa from the Riess et al. (2004) gold sample (157 minus the 37 low-redshift objects in common) and 115 SNeIa from Astier et al. (2006).

The two SNIa studies use different light curve fitting methods. In order to compare and combine the data, we fit the observed distance moduli $\mu^{\rm obs}(z_{\rm i}) = m^{\rm obs}(z_{\rm i}) - M$, where m is the apparent magnitude at maximum light after applying galactic extinction, K-correction and light curve width–luminosity corrections, and M is the absolute magnitude, with the theoretical predictions, $\mu^{\rm th}(z_{\rm i}) = m^{\rm th}(z_{\rm i}) - M = 5\,\log_{10}D_{\rm L}(z_{\rm i};\theta) + \mu_0$, where $D_{\rm L} = H_0\,d_{\rm L}$ is the H_0-free luminosity distance, $\mu_0 = 25 - 5\,\log_{10}H_0$ and $m_0 \equiv M + \mu_0$ is a 'nuisance parameter' which contains both the absolute magnitude and H_0.

For the $[q_0,\, j(a;\mathcal{C})]$ parameter space, the luminosity distance $d_{\rm L}(z;\theta)$ is directly obtained integrating the solution of the differential equation (7) with the definition (11) as presented in Section 2.2. For models using linear parametrization of $q(z)$ and/or dynamical models with $\Omega_{\rm m}$ and w, we plug equations (1) and (12), respectively, into the equation describing the luminosity distance for a flat FRWL metric, in units of megaparsecs:

$$d_{\rm L}(z;\theta) = \frac{c(1+z)}{H_0}\int_0^z \frac{{\rm d}z}{E(z;\theta)}, \tag{19}$$

where the speed of light, c, is in km s^{-1} and the present Hubble parameter, H_0, in km (s Mpc)$^{-1}$. Here, the vectors of parameters for each model are $\theta = (q_0,\, {\rm d}q/{\rm d}z)$ and $\theta = (\Omega_{\rm m},\, w)$. For the gold sample data of Riess et al. (2004), we use the extinction-corrected distance moduli, $\mu^{\rm obs}(z_{\rm i})$ and associated errors, $\sigma_{\rm i}^2$. For the SNLS data of Astier et al. (2006), we use the rest-frame B-band magnitude at maximum light $m_B^*(z_{\rm i})$, the stretch factor $s_{\rm i}$ and the rest-frame colour $c_{\rm i}$ to obtain $\mu^{\rm obs}(z_{\rm i}) = m_B^*(z_{\rm i}) - M + \alpha\,(s_{\rm i} - 1) - \beta c_{\rm i}$. These values were derived from the light curves by Astier et al. (2006), who also provided best-fitting values for $\alpha = 1.52 \pm 0.14$ and $\beta = 1.57 \pm 0.15$.

For both SNIa data sets, we have

$$\chi^2(\theta; m_0) = \sum_{\rm SNIa}\frac{\left[\mu^{\rm th}(z_{\rm i};\theta,\,\mu_0) - \mu^{\rm obs}(z_{\rm i};\theta,\,M)\right]^2}{\sigma_{\rm i}^2}, \tag{20}$$

where the dispersion associated with each data point, $\sigma_{\rm i}^2 = \sigma_{\mu_{\rm i,obs}}^2 + \sigma_{\rm int,i}^2 + \sigma_{\rm v,i}^2$. Here $\sigma_{\mu_{\rm i,obs}}^2$ accounts for flux uncertainties, $\sigma_{\rm int,i}^2$ accounts for intrinsic, systematic dispersion in SNIa absolute magnitudes and $\sigma_{\rm v,i}^2$ accounts for systematic scatter due to peculiar velocities. The SNLS analysis includes an intrinsic dispersion of 0.131 04 mag[4] and a peculiar velocity scatter of 300 km s^{-1}. The gold sample analysis includes 400 km s^{-1} peculiar velocity scatter, with an additional 2500 km s^{-1} added in quadrature for high-redshift SNeIa.

We marginalize analytically over m_0:

$$\tilde{\chi}^2(\theta) = -2\ln\int_{-\infty}^{\infty}\exp\left[-\frac{1}{2}\chi^2(\theta, m_0)\right]{\rm d}m_0 \tag{21}$$

obtaining

$$\tilde{\chi}^2 = \ln\left(\frac{c}{2\pi}\right) + a - \frac{b^2}{c}, \tag{22}$$

where

$$a = \sum_{\rm SNIa}\frac{\left[5\log_{10}D_{\rm L}(z_{\rm i};\theta) - m^{\rm obs}(z_{\rm i})\right]^2}{\sigma_{\rm i}^2}, \tag{23}$$

$$b = \sum_{\rm SNIa}\frac{5\log_{10}D_{\rm L}(z_{\rm i};\theta) - m^{\rm obs}(z_{\rm i})}{\sigma_{\rm i}^2}, \qquad c = \sum_{\rm SNIa}\frac{1}{\sigma_{\rm i}^2}. \tag{24}$$

Note that the absolute value of $\chi^2 = a - (b^2/c)$. For the analysis in the standard dynamic framework, our results agree with those of Riess et al. (2004) and Astier et al. (2006), and the comparison work of Nesseris & Perivolaropoulos (2005).

4.2 X-ray cluster data

For the analysis of cluster X-ray gas mass fractions, we use the data of Allen et al. (in preparation), which contain 41 X-ray-luminous, relaxed galaxy clusters, including 26 previously studied by Allen et al. (2004). [Some of the original 26 have since been revisited by the *Chandra X-ray Observatory* leading to improved constraints (for details see Allen et al., in preparation)]. The new X-ray data set spans a redshift interval $0.06 < z < 1.07$. Our analysis follows the method of Allen et al. (2004), fitting the apparent redshift evolution of the cluster gas fraction with the expression

$$f_{\rm gas}^{\rm ref}(z_{\rm i}) = \mathcal{F}\,R^{\rm ref}(z_{\rm i}), \quad R^{\rm ref}(z_{\rm i}) \equiv \left[\frac{d_{\rm A}^{\rm ref}(z_{\rm i})}{D_{\rm A}(z_{\rm i})}\right]^{1.5}, \tag{25}$$

where $\mathcal{F} = (b\,\Omega_{\rm b}H_0^{1.5})/[(1 + 0.19\sqrt{h})\,\Omega_{\rm m}]$ is the normalization of the $f_{\rm gas}(z)$ curve, $d_{\rm A}$ and $d_{\rm A}^{\rm ref}\,(z)$ are the angular diameter distances $[d_{\rm A} = d_{\rm L}/(1+z)^2]$ to the clusters for a given cosmology and for the reference ΛCDM cosmology [with $H_0 = 70$ km (s Mpc)$^{-1}$ and $\Omega_{\rm m} = 0.3$], respectively, and $D_{\rm A} = H_0\,d_{\rm A}$ is the H_0-free angular diameter distance. For the kinematical approach, we treat the normalization $\mathcal{F}$ as a single 'nuisance' parameter, which we marginalize over in the MCMC chains.

For the *dynamical* analysis of the same X-ray data, we follow Allen et al. (2004) and employ Gaussian priors on the present value of the Hubble parameter $H_0 = 72 \pm 8$ km (s Mpc)$^{-1}$ (Freedman et al. 2001), the mean baryon density $\Omega_{\rm b}\,h^2 = 0.0214 \pm 0.0020$ (Kirkman et al. 2003) and the X-ray bias factor $b = 0.824 \pm 0.089$ [determined from the hydrodynamical simulations of Eke, Navarro & Frenk (1998), including a 10 per cent allowance for systematic uncertainties]. The application of these priors leads to an additional constraint on $\Omega_{\rm m}$ from the normalization of the $f_{\rm gas}(z)$ curve. Since the kinematical approach does not constrain $\Omega_{\rm m}$, the kinematical analysis does not involve these priors and draws information only from the shape of the $f_{\rm gas}(z)$ curve. The dynamical analysis, in constrast, extracts information from both the shape *and* the normalization.

4.3 Markov Chain Monte Carlo analysis

For both the kinematical and the dynamical analyses, we sample the posterior probability distributions for all parameter spaces using an MCMC technique. This provides a powerful tool for cosmological studies, allowing the exploration of large multidimensional

[2] Riess et al. (2004) presented 16 new *Hubble Space Telescope* (*HST*) SNeIa, combined with 170 previously reported SNeIa from ground-based data. They identified a widely used 'high-confidence' subset, usually referred to as the *gold sample*, which includes 14 *HST* SNeIa.

[3] 71 SNLS objects, plus 44 previously reported nearby objects.

[4] http://snls.in2p3.fr/conf/papers/cosmo1/.

parameter spaces. In detail, we use the Metropolis–Hastings algorithm implemented in the COSMOMC[5] code of Lewis & Bridle (2002) for the dynamic formalism, and a modified version of this code for the kinematic analysis.

Our analysis uses four MCMC chains for each combination of model and data. We ensure convergence by applying the Gelman–Rubin criterion (Gelman & Rubin 1992), where the convergence is deemed acceptable if the ratio of the between-chain and mean-chain variances satisfies $R - 1 < 0.1$. In general, our chains have $R - 1 \ll 0.1$.

4.4 Hypothesis testing in the kinematical analysis: how many model parameters are required?

In the first case, we examined a kinematical model in which the deceleration parameter q_0 was included as the only interesting free parameter [see equation (1) with $q' = 0$]. This is hereafter referred to as the model $\mathcal{Q}$. As detailed in Section 2, we next introduced the jerk parameter, j, as an additional free parameter, allowing it to take any constant value. We refer to this as model $\mathcal{J}$, which has the interesting free parameters, q_0 and j. Note that model $\mathcal{J}$ includes the set of possible ΛCDM models, which all have constant $j = 1$.

We next explored a series of models that allow for progressively more complicated deviations from ΛCDM. In each case, the improvement obtained with the introduction of additional model parameters, has been gauged from the MCMC chains using a variety of statistical tests. In the first case, we follow a frequentist approach and use the F-test, for which

$$F = \frac{\Delta\chi^2}{\chi^2_\nu\, \Delta m}, \tag{26}$$

where $\Delta\chi^2$ is the difference in the minimum χ^2 between the two models, χ^2_ν is the reduced χ^2 (χ^2/ν, where ν is the number of degrees of freedom of the fit, d.o.f.) of the final model, and Δm is the difference in the number of free parameters in the two models. Given Δm and ν, we calculate the probability that the new model would give $\Delta\chi^2 \geqslant F\,\chi^2_\nu\,\Delta m$ by random chance. This allows us to quantify the significance of the model extension.

The Bayesian Information Criterion (BIC) provides a more stringent model selection criterion and is an approximation to the Bayesian Evidence (Schwarz 1978). The BIC is defined as

$$\mathrm{BIC} = -2\ln\mathcal{L} + k\ln N, \tag{27}$$

where $\mathcal{L}$ corresponds to the maximum likelihood obtained for a given model (thus, $-2\ln\mathcal{L}$ is the minimum χ^2), k is the number of free parameters in the model and N is the number of data points. Values for $\Delta\mathrm{BIC} < 2$ between two models are typically considered to represent weak evidence for an improvement in the fit. ΔBIC between 2 and 6 indicates 'positive evidence' for an improvement, and values greater than 6 signify 'strong evidence' for the model with the higher BIC (Jeffreys 1961; Kass & Raftery 1995; Mukherjee et al. 1998; Liddle 2004).

Finally, we have compared the full posterior probability distributions for different models, using the Bayes factor to quantify the significance of any improvement in the fit obtained. The Bayes factor is defined as the ratio between the Bayesian evidence of the two models (Kass & Raftery 1995). If $P(D|\theta, M)$ is the probability of the data D given a model M, the Bayesian evidence is defined as the integral over the parameter space, θ:

$$E(M) \equiv P(D|M) = \int \mathrm{d}\theta\, P(D|\theta, M)\, P(\theta|M), \tag{28}$$

where $P(\theta|M)$ is the prior on the set parameters θ, normalized to unity. We employ top hat priors for all parameters and evaluate the integrals using the MCMC samples:

$$E(M) \sim \frac{1}{N\Delta\theta}\sum^{N} P(D|\theta_n), \tag{29}$$

where $\Delta\theta$ is the volume in the parameter space selected to have probability 1 within the top hat priors, N is the number of MCMC samples and θ_n the sampled parameter space. Note that $\sum^N P(D|\theta_n)$ is the expected probability of the data in the posterior distribution (Lewis & Bridle 2002). The evidence of the model $E(M)$ can be estimated trivially from the MCMC samples as the mean likelihood of the samples divided by the volume of the prior. It is clear, though, that this volume will depend on our selection of the top hat priors. In order to be as objective as possible, within the Bayesian framework, we use the same priors for parameters in common between the two models involved in a comparison. For parameters not in common, we calculate their volumes subtracting their maximum and minimum values in the MCMC samples.

The Bayes factor between the two models M_0 and M_1 is $B_{01} = E(M_0)/E(M_1)$. If $\ln B_{01}$ is positive, M_0 is 'preferred' over M_1. If $\ln B_{01}$ is negative, M_1 is preferred over M_0. Following the scale of Jeffreys (1961), if $0 < \ln B_{01} < 1$ only a 'bare mention' of the preference is considered warranted. If $1 < \ln B_{01} < 2.5$, the preference is regarded as of 'substantial' significance. If $2.5 < \ln B_{01} < 5$, the significance is considered to be going from 'strong' to 'very strong'.

5 RESULTS

5.1 Comparison of constant jerk and constant w models

We first examine the statistical improvement obtained in moving from the simplest kinematical model $\mathcal{Q} = [q_0]$, in which q_0 is the only interesting free parameter, to model $\mathcal{J} = [q_0, j(c_0)]$, where we include constant jerk $j = 1 + c_0$ (i.e. we allow j to take values other than zero). The results obtained, using the three statistical tests described in Section 4.1 applied to each data set alone and for all three data sets together, are summarized in Table 1. We find that the 'gold' sample is the only data set that, on its own, indicates a 'substantial' preference for model $\mathcal{J}$ over model $\mathcal{Q}$ according to the Bayes factor test. Note that this is not only due to the fact that the 'gold' sample extends to higher redshifts, thereby providing additional constraining power, but also due to the fact that the 'gold' sample hints a small tension in the ground-based 'gold' sample data to prefer $j > 1$ values.[6] Combining all three data sets, we obtain a 'strong' preference for model $\mathcal{J}$ over model $\mathcal{Q}$, from all three statistical tests. Table 1 shows the mean marginalized parameters for each model and the 1σ confidence levels. Combining all three data sets, we obtain tight constraints on $q_0 = -0.81 \pm 0.14$ and

[5] http://cosmologist.info/cosmomc/.

[6] An analysis of the 'gold' sample data in which the *HST* SNeIa are excluded leads to even stronger preference for $j > 0$: $\Delta\chi^2_{\mathcal{J}\mathcal{Q}} = 10.6$. In this case, for model $\mathcal{J}$ we obtain $q_0 = -1.17 \pm 0.28$ and $j = 4.95^{+2.05}_{-1.84}$.

Table 1. The marginalized median values and 68.3 per cent confidence intervals obtained by analysing each data set and all three data sets together. We show these results for two kinematical models: using only q_0($\mathcal{Q}$ model) and extending this parameter space with the jerk parameter j ($\mathcal{J}$ model). We quote χ^2 per d.o.f. for each model and three different statistical tests to quantify the significance of extending the parameter space from $\mathcal{Q}$ (q_0) to $\mathcal{J}$ (q_0, j). We quote the difference in $\Delta\chi^2_{\mathcal{J}\mathcal{Q}}$, the probability given by F-test, the difference in the BIC and $\ln B_{\mathcal{J}\mathcal{Q}}$ (where $B_{\mathcal{J}\mathcal{Q}}$ is the Bayes factor between the two models). Note that combining all three data sets we obtain a significant preference for the $\mathcal{J}$ model within all three tests.

Data set	$\mathcal{Q}$ model		$\mathcal{J}$ model				Improvement		
	q_0	$\chi^2_{\mathcal{Q}}$/d.o.f.	q_0	j	$\chi^2_{\mathcal{J}}$/d.o.f.	$\Delta\chi^2_{\mathcal{J}\mathcal{Q}}$	F-test (per cent)	ΔBIC	$\ln B_{\mathcal{J}\mathcal{Q}}$
Clusters	-0.55 ± 0.14	39.6/39	$-0.61^{+0.38}_{-0.41}$	$0.51^{+2.55}_{-2.00}$	39.6/38	0.01	5.6	-3.7	-3.2
SNLS SNeIa	-0.417 ± 0.062	112.1/113	-0.65 ± 0.23	$1.32^{+1.37}_{-1.21}$	111.0/112	1.1	69.4	-3.6	-2.5
Gold SNeIa	-0.289 ± 0.062	182.8/155	-0.86 ± 0.21	$2.75^{+1.22}_{-1.10}$	174.6/154	8.2	99.1	3.1	1.2
Gold+SNLS+Cl	-0.391 ± 0.045	300.8/272	-0.81 ± 0.14	$2.16^{+0.81}_{-0.75}$	290.1/271	10.7	99.8	5.1	3.0

Table 2. The marginalized median values and 68.3 per cent confidence intervals obtained analysing all three data sets together. We show the results for the constant j model (kinematical) and the constant w model (dynamical) and their corresponding χ^2 per d.o.f.

Approach	Model parameters	χ^2/d.o.f.
Kinematical	$q_0 = -0.81 \pm 0.14$, $j = 2.16^{+0.81}_{-0.75}$	290.1/271
Dynamical	$\Omega_{\rm m} = 0.306^{+0.042}_{-0.040}$, $w = -1.15^{+0.14}_{-0.18}$	291.7/272

$j = 2.16^{+0.81}_{-0.75}$. Our result represents the first measurement of the jerk parameter from cosmological data.[7]

Our dynamical analysis of the same three data sets gives $w = -1.15^{+0.14}_{-0.18}$ and $\Omega_{\rm m} = 0.306^{+0.042}_{-0.040}$ (see Table 2). Fig. 1 shows the constraints for both the kinematical (q_0, j; top left-hand panel) and the dynamical ($\Omega_{\rm m}$, w; top right-hand panel) models, using all three data sets combined. In both cases, the dashed lines indicate the expected range of results for ΛCDM models (i.e. a cosmological constant). We find that both the kinematical and the dynamical analyses of the combined data are consistent with the ΛCDM model at about the 1σ level.

It is important to recognize that the results from the kinematical and dynamical analyses constrain different sets of departures from ΛCDM. We are using two simple, but very different parametrizations based on different underlying assumptions. The results presented in Fig. 1 therefore provide interesting new support for the ΛCDM model.

The lower panels of Fig. 1 show the constraints obtained for the three data sets when analysed individually. It is important to note the consistent results from the independent SNIa and X-ray cluster data sets. Note that in the dynamical analysis, the X-ray data provide valuable additional constraints on $\Omega_{\rm m}$, when employing the H_0 and $\Omega_{\rm b}h^2$ priors. The overlap of all three data sets in both parameter spaces highlights the robustness of the measurements. Comparing the upper and lower panels of Fig. 1, we see how the combination of data sets significantly tightens the constraints.

5.2 More-complicated kinematical models

For the combined data set, we have also searched for more-complicated departures from ΛCDM by including extra model parameters, as described in Section 3. We find no significant evidence for models more complicated than a constant jerk model. In particular, we find a negligible $\Delta\chi^2$ between models with constant jerk $\mathcal{J} = [q_0, j(c_0)]$ and the next most-sophisticated model $\mathcal{J}_1 = [q_0, j(a; c_0, c_1)]$, and between the latter model and the next one, $\mathcal{J}_2 = [q_0, j(a; c_0, c_1, c_2)]$.

It is, however, interesting to plot the differences between the constraints obtained for each model. Fig. 2 shows the current 1 and 2σ constraints around the median values of $j(a)$ at different scalefactors, a, over the range where we have data [0.36, 1]. The green, lighter contours show the constraints for the $\mathcal{J}_1$ model and the red, darker contours for the $\mathcal{J}$ model. From this figure, it is clear that current data provide the best constraints around $a \sim 0.77$, that is, $z \sim 0.3$, and that at higher and lower redshift more data are required. For the low-redshift range, the forthcoming SDSS II SNIa data will be helpful. For the high-redshift range, new *HST* SNIa and further X-ray cluster data should be available in the near future. In the longer term, SNIa data from the Large Synaptic Survey Telescope (LSST),[8] the Supernovae Acceleration Probe (SNAP),[9] and X-ray cluster data from Constellation-X[10] should provide tight constraints on both $j(a)$ and $w(a)$. Future galaxy redshift surveys covering a high-redshift range will also help us to tighten these constraints, using the baryon oscillation experiment (Cole et al. 2005; Eisenstein et al. 2005).

5.3 Comparison of distance measurements

It is interesting to compare directly the distance curves for the kinematical (constant j) and dynamical (constant w) models, as determined from the MCMC chains. Fig. 3 shows the 68.3 and 95.4 per cent confidence limits on the offset in distance, as a function of scalefactor, relative to a reference ΛCDM cosmology with $\Omega_{\rm m} = 0.27, \Omega_\Lambda = 0.73$. We see that the kinematical and dynamical results occupy very similar, though not identical, loci in the distance–scalefactor plane. For the dynamical analysis, the addition of the extra constraint on $\Omega_{\rm m}$ from the normalization of the $f_{\rm gas}$ curve tightens the constraints and pushes the results in a direction slightly more consistent with the reference ΛCDM cosmology.

5.4 Comparison with Riess et al. (2004)

For comparison purposes, we also present the results obtained using the linear parametrization of $q(z)$ described by

[7] Note that Riess et al. (2004) measured $j_0 > 0$ at the 2σ level, where j_0 comes from a Taylor expansion of the Hubble parameter around small redshifts (Visser 2004). As noted in Section 2.1 such an expansion is not appropriate when high-redshift data are included, as in the 'gold' sample.

[8] http://www.lsst.org/lsst_home.shtml.

[9] http://snap.lbl.gov/.

[10] http://constellation.gsfc.nasa.gov/.

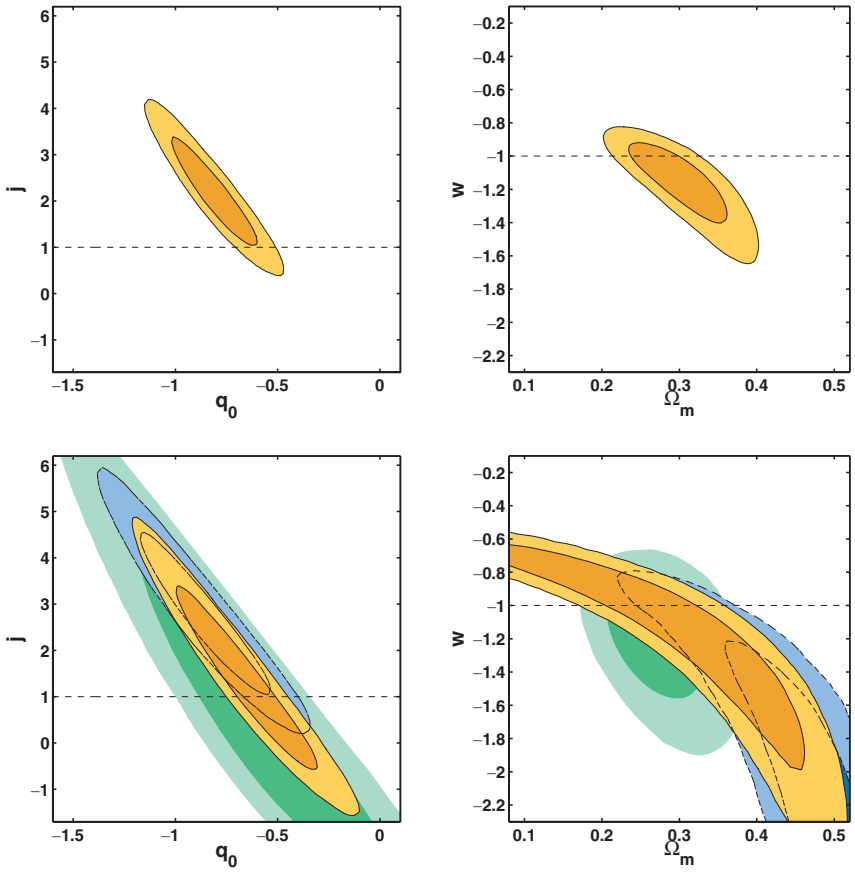

Figure 1. A summary of the results from the kinematical (left-hand panels) and the dynamical (right-hand panels) analyses. The top left-hand panel shows the 68.3 and 95.4 per cent confidence limits in the (q_0, j) plane for the kinematical model with a constant jerk, j, obtained using all three data sets: both the SNIa data sets (Riess et al. 2004; Astier et al. 2006) and the cluster $f_{\rm gas}$ data of Allen et al. (in preparation). The top right-hand panel shows the results in the $(\Omega_{\rm m}, w)$ plane obtained using the same three data sets and assuming *HST*, BBNS and b priors. (Note that the kinematical analysis does not use the *HST*, BBNS and b priors.) The dashed lines show the expectation for a cosmological constant model in both formalisms ($j = 1$ and $w = -1$, respectively). The bottom panels show the confidence contours in the same planes for the individual data sets: the SNLS SNIa data (orange contours), the Riess et al. (2004) 'gold' SNIa sample (blue contours) and the cluster $f_{\rm gas}$ data (green contours). Here, the dashed lines again indicate the cosmological constant model.

equation (3) and used by Riess et al. (2004). Fig. 4 shows the constraints in the plane $(q_0, {\rm d}q/{\rm d}z)$ determined from each data set, and by combining the three data sets (solid, orange contours). It is clear that the constraints from the three independent data sets overlap and that by combining them we obtain significantly tighter results than using the 'gold' sample alone.

6 THE DISTANCE TO THE LAST SCATTERING SURFACE

Finally, we note that there is one further pseudo-distance measurement available to us – the distance to the last scattering surface from CMB data. Although this is not a purely kinematical data point, for illustration purposes we show the constraints on $j(a)$ that can be achieved if one is willing to make extra assumptions and include this measurement. The extra assumptions involved, though strong, are well motivated. In detail, in order to use the distance to last scattering, we assume that dark matter behaves like standard CDM at all redshifts, an assumption well tested by, for example, galaxy cluster, weak-lensing and galaxy redshift surveys at low redshifts and CMB experiments at high redshift. We also assume that pre-recombination physics can be well described by a standard combination of CDM, a photon-baryon fluid and neutrinos, and that any early dark energy component has a negligible effect on the dynamics. With these assumptions, one can construct the comoving angular diameter distance to the last scattering surface from $d_{\rm A} = r_{\rm s}(a_{\rm dec})/\theta_{\rm A}$, where $r_{\rm s}(a_{\rm rec})$ and $\theta_{\rm A}$ are the comoving sound horizon at decoupling and the characteristic angular scale of the acoustic peaks, respectively. For a geometrically flat Universe with a negligible early dark energy component, we calculate the sound horizon at decoupling as (Verde et al. 2003):

$$r_{\rm s}(a_{\rm dec}) \simeq \int_0^{a_{\rm dec}} \frac{c_{\rm s}(a)}{H_0(\Omega_{\rm m}a + \Omega_{\rm rad})^{1/2}}\,{\rm d}a, \qquad (30)$$

where $c_{\rm s}(a) = c/[1 + (3\Omega_{\rm b}\ a)/(4\Omega_\gamma)]$ is the sound speed in the photon-baryon fluid, $\Omega_{\rm rad} = \Omega_\gamma + \Omega_\nu$ is the present radiation energy density, and Ω_γ and Ω_ν are the present photon and neutrino energy densities, respectively. We use our X-ray galaxy cluster data, assuming *HST*, BBNS and b priors, to determine $\Omega_{\rm m} = 0.27 \pm 0.04$ (Allen et al., in preparation; note that this constraint mainly comes from low-redshift clusters). We also use the *COBE* measurement of the CMB temperature $T_0 = 2.725 \pm 0.002$K (Mather et al. 1999) and a standard three neutrino species model with negligible masses to obtain $\Omega_{\rm rad}$. For these constraints, we obtain $r_{\rm s}(z_{\rm dec}) \simeq 146 \pm 10$ Mpc.

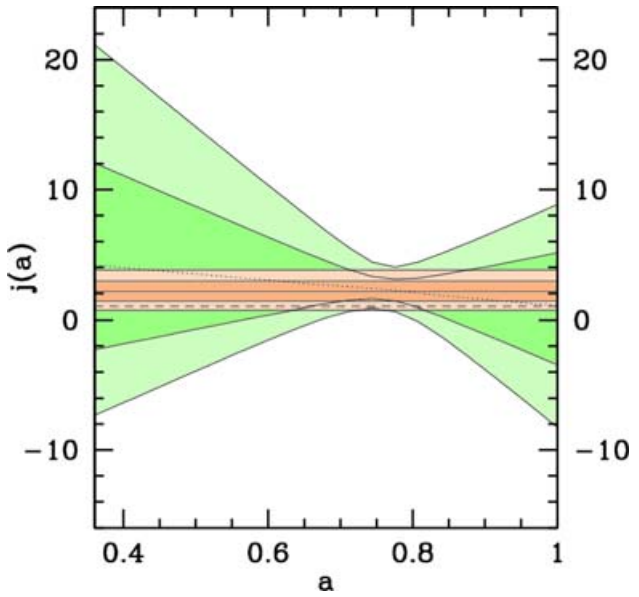

Figure 2. The 68.3 and 95.4 per cent confidence variations about the median values for $j(a)$ as a function of the scalefactor a, over the range where we have data [0.36, 1]. Results are shown for the constant jerk model (model $\mathcal{J}$) (red, darker contours) and $\mathcal{J}_1$ model (green, lighter contours). In both cases, the constraints for all three data sets have been combined. The dashed line indicates the expectation, $j = 1$ (constant) for a cosmological constant (ΛCDM) model.

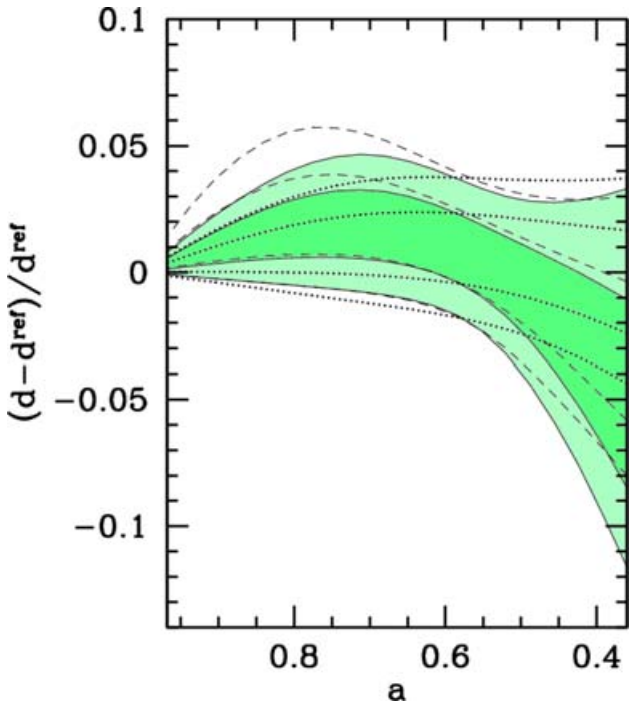

Figure 3. The 68.3 and 95.4 per cent confidence limits on the offset in distance as a function of scalefactor, relative to the reference ΛCDM cosmology, for both the kinematical (constant j; green, shaded curves) and the dynamical (constant w; dotted and dashed curves) analyses. The dotted curves show the results for the dynamical analysis in which the additional constraint on $\Omega_{\rm m}$ from the normalization of the $f_{\rm gas}$ curve is used. The dashed curve is for a dynamical analysis where this extra constraint on the normalization is ignored. The same MCMC samples as used to construct Fig. 1 have been used.

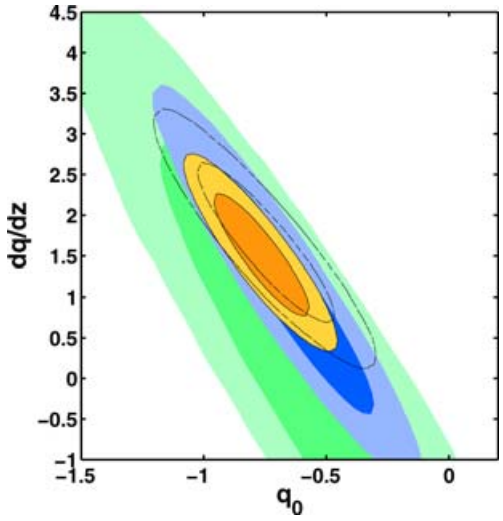

Figure 4. The 68.3 and 95.4 per cent confidence limits in the $(q_0, {\rm d}q/{\rm d}z)$ plane obtained using the SNIa data from the first year of the SNLS (Astier et al. 2006) (blue contours), the 'gold' sample of Riess et al. (2004) (dashed contours), the cluster $f_{\rm gas}$ data of Allen et al. (in preparation) (green contours) and the combination of all three data sets (orange contours).

From Hinshaw et al. (2006), we have the multipole of the first acoustic peak $l_1 = 220.7 \pm 0.7$. This is related to $l_{\rm A}$ by a shift ϕ, $l_1 = l_{\rm A}(1 - \phi)$. Using the fitting formula of Doran & Lilley (2002), the BBNS prior for $\Omega_{\rm b}h^2$, a scalar spectral index $n_{\rm s} = 0.95 \pm 0.02$ (Spergel et al. 2006) and assuming no early dark energy, we find $\theta_{\rm A} = 0.^{\circ}6 \pm 0.^{\circ}01$. We then obtain a pseudo-model-independent distance to decoupling, $d(z_{\rm dec}) \simeq 13.8 \pm 1.1$ Gpc, where $z_{\rm dec} = 1088$ (Spergel et al. 2006).

Fig. 5 shows the tightening of the constraints obtained using this 'data-point-prior' at high redshift.[11] Note that Fig. 5 is plotted on the same scale as Fig. 2 and shows $\mathcal{J}$ (red, darker contours) and $\mathcal{J}_1$ (green, lighter contours) models as before, plus the $\mathcal{J}_2$ model (blue contours). Note also that here the range of the data is [$a_{\rm min} = 0.0009$, $a_{\rm max} = 1$]. Again, using equation (15) we rescale the Chebyshev interval $[-1, 1]$ to locate the functions $\Delta j(a; \mathcal{C})$ in the range of scalefactor spanned by the data. The prior information at high redshift, from the distance to last scattering, tightens the constraints significantly. Evidently, the constraints from the kinematic analysis are sensitive to the data quality at high redshift.

7 CONCLUSIONS

We have developed a new kinematical approach to study the expansion of the history of the Universe, building on the earlier work of Blandford et al. (2004). Our technique uses the parameter space defined by the current value of the cosmic deceleration parameter q_0 and the jerk parameter j, where q and j are the dimensionless second and third derivatives of the scalefactor with respect to cosmic time.

[11] Note that extending the analysis to the decoupling redshift $z_{\rm dec} = 1088$ means that the radiation density becomes non-negligible. Although, j can still be calculated as usual, $j^{\Lambda{\rm CDM}}$ will not be equal to 1 at these redshifts. However, the ΛCDM model can then be almost perfectly described as $j^{\Lambda{\rm CDM}}(a) = 1 + 2/[1 + (a/a_{\rm eq})]$ (see for details Amin & Blandford, in preparation), where $a_{\rm eq}$ is the mean marginalized scalefactor at equality, from *WMAP* data. We have explicitly verified that, within the 1σ values of $a_{\rm eq}$, systematic offsets due to the effects of radiation have a negligible effect on the derived distances.

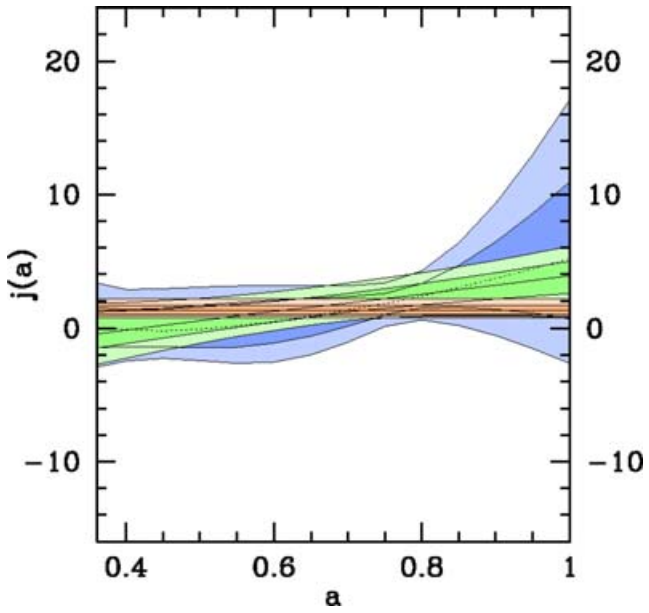

Figure 5. 1 and 2σ constraints on $j(a)$ over the range (including the distance to the last scattering surface) of the data [0.0009, 1]. Note that this figure and Fig. 2 are plotted on the same scale for comparison purposes. This figure shows the same models as shown in Fig. 2 plus the $\mathcal{J}_2$ model, and uses the CMB prior as described in the text. The dotted line shows the median $j(a)$ curve for the $\mathcal{J}_1$ model.

The use of this (q_0, j) parameter space provides a natural framework for kinematical studies. In particular, it provides a simple prescription for searching for departures from ΛCDM, since the complete set of ΛCDM models are characterized by $j = 1$ (constant).

We have applied our technique to the three best available sets of redshift-independent distance measurements, from SNIa studies (Riess et al. 2004; Astier et al. 2006) and measurements of the X-ray gas mass fraction in X-ray luminous, dynamically relaxed galaxy clusters (Allen et al., in preparation). Assuming geometric flatness, we measure $q_0 = -0.82 \pm 0.14$ and $j = 2.16^{+0.81}_{-0.75}$ (Fig. 1). Note that this represents the first measurement of the cosmic jerk parameter, j. A more standard, dynamical analysis of the same data gives $w = -1.15^{+0.14}_{-0.18}$ and $\Omega_{\rm m} = 0.306^{+0.042}_{-0.040}$, also assuming flatness and *HST*, BBNS and b priors (Fig. 1). Both sets of results are consistent with the standard ΛCDM paradigm, at about the 1σ level.

In comparison to standard, dynamical approaches, our kinematical framework provides a different set of simple models and involves fewer assumptions. In particular, kinematical analyses such as that presented here do not assume a particular gravity theory. The combination of the kinematical and dynamical approaches therefore provides important, complementary information for investigating late-time cosmic acceleration. The fact that both the kinematical and the dynamical results presented here are consistent with ΛCDM provides important additional support for that model. The fact that the two independent sets of distance measurements, from X-ray galaxy clusters and SNe, are individually consistent with ΛCDM, is reassuring (Fig. 1).

We have searched for departures from ΛCDM using a new scheme based on the introduction of Chebyshev polynomials. These orthonormal functions allow us to expand any deviation from ΛCDM, $\Delta j(a; \mathcal{C})$, as a linear combination of polynomials. We use the coefficients of these polynomials, $\mathcal{C}$, as fit parameters. The current data provide no evidence for a dependence of j on a more complicated than a constant value. However, higher-order terms may be required to describe future data sets. In that case, our scheme has the advantage that, over a finite interval and using enough high-order terms, it will provide an acceptable global approximation to the true underlying shape. Note that this scheme is also applicable to dynamical studies of the evolution of the dark energy equation-of-state, $w(a)$. Note also that Chebyshev polynomial expansions of the same order for $w(a)$ and $j(a)$ explore a different set of models. For example, a constant $j \neq 1$ model corresponds to an evolving $w(a)$ model and vice versa.

We suggest that future studies should endeavour to use both kinematical and dynamical approaches where possible, in order to extract maximum information from the data. The two approaches have different strengths, can be applied to a variety of data sets, and are highly complementary. The combination of techniques may be especially helpful in distinguishing an origin for cosmic acceleration that lies with dark energy (i.e. a new energy component to the Universe) from modifications to General Relativity.

ACKNOWLEDGMENTS

We acknowledge helpful discussions with A. Frolov and technical support from G. Morris. The computational analysis was carried out using the KIPAC XOC compute cluster at the SLAC. SWA acknowledges support from the National Aeronautics and Space Administration (NASA) through Chandra Award Number DD5-6031X issued by the Chandra X-ray Observatory Centre, which is operated by the Smithsonian Astrophysical Observatory for and on behalf of the NASA under contract NAS8-03060. RDB acknowledges support from National Science Foundation grant AST05-07732. This work was supported in part by the US Department of Energy under contract number DE-AC02-76SF00515.

REFERENCES

Alam U., Sahni V., Saini T. D., Starobinsky A. A., 2003, MNRAS, 344, 1057
Allen S. W., Schmidt R. W., Fabian A. C., 2002, MNRAS, 334, L11
Allen S. W., Schmidt R. W., Fabian A. C., Ebeling H., 2003, MNRAS, 342, 287
Allen S. W., Schmidt R. W., Ebeling H., Fabian A. C., van Speybroeck L., 2004, MNRAS, 353, 457
Armendariz-Picon C., Mukhanov V., Steinhardt P. J., 2000, Phys. Rev. Lett., 85, 4438
Armendariz-Picon C., Mukhanov V., Steinhardt P. J., 2001, Phys. Rev. D, 63, 103510
Astier P. et al., 2006, A&A, 447, 31
Bagla J. S., Jassal H. K., Padmanabhan T., 2003, Phys. Rev. D, 67, 063504
Barreiro T., Copeland E. J., Nunes N. J., 2000, Phys. Rev. D, 61, 127301
Bento M. C., Bertolami O., Sen A. A., 2002, Phys. Rev. D, 66, 043507
Blandford R. D., Amin M., Baltz E. A., Mandel K., Marshall P. J., 2004, in Wolff S. C., Lauer T. R., eds, ASP Conf. Ser. 339, Observing Dark Energy. Astron. Soc. Pac., San Francisco, p. 27
Borgani S. et al., 2001, ApJ, 561, 13
Cabre A., Gaztanaga E., Manera M., Fosalba P., Castander F., 2006, MNRAS, 372, L23
Caldwell R. R., Doran M., 2005, Phys. Rev. D, 72, 043527
Caldwell R. R., Kamionkowski M., 2004, JCAP, 0409, 009
Caldwell R., Dave R., Steinhardt P., 1998, Phys. Rev. Lett., 80, 1582
Capozziello S., Carloni S., Troisi A., 2003, preprint (astro-ph/0303041)
Carroll S. M., Hoffman M., Trodden M., 2003, Phys. Rev. D, 68, 023509
Carroll S. M., Duvvuri V., Trodden M., Turner M. S., 2004, Phys. Rev. D, 70, 043528
Carroll S. M., de Felice A., Duwuri V., Easson D. A., Trodden M., Turner M. S., 2005, Phys. Rev. D, 71, 063513

Chiba T., Nakamura T., 1998, Prog. Theor. Phys., 100, 1077
Chiba T., Okabe T., Yamaguchi M., 2000, Phys. Rev. D, 62, 023511
Cole S. et al., 2005, MNRAS, 362, 505
Copeland E. J., Liddle A. R., Wands D., 1998, Phys. Rev. D, 57, 4686
Copeland E. J., Garousi M. R., Sami M., Tsujikawa S., 2005, Phys. Rev. D, 71, 043003
Copeland E. J., Sami M., Tsujikawa S., 2006, Int. J. Modern Phys. D, 15, 1753
Corasaniti P. S., Kunz M., Parkinson D., Copeland E. J., Bassett B. A., 2004, Phys. Rev. D, 70, 083006
Croft R. A. C., Weinberg D. H., Bolte M., Burles S., Hernquist L., Katz N., Kirkman D., Tytler D., 2002, ApJ, 581, 20
Deffayet C., Dvali G., Gabadadze G., 2002a, Phys. Rev. D, 65, 044023
Deffayet C., Landau S. J., Raux J., Zaldarriaga M., Astier P., 2002b, Phys. Rev. D, 66, 024019
Doran M., Lilley M., 2002, MNRAS, 330, 965
Dvali G. R., Gabadadze G., Porrati M., 2000, Phys. Lett., B485, 208
Eisenstein D. J. et al., 2005, ApJ, 633, 560
Eke V. R., Navarro J. F., Frenk C. S., 1998, ApJ, 503, 569
Elgaroy O., Multamaki T., 2006, JCAP, 0609, 002
Ettori S., Tozzi P., Rosati P., 2003, A&A, 398, 879
Fosalba P., Gaztanaga E., Castander F., 2003, ApJ, 597, L89
Freedman W. et al., 2001, ApJ, 553, 47
Gelman A., Rubin D. B., 1992, Statis. Sci., 7, 457
Gong Y., Wang A., 2006, Phys. Rev. D, 73, 083506
Guo Z.-K., Zhu Z.-H., Alcaniz J. S., Zhang Y.-Z., 2006, ApJ, 646, 1
Hinshaw G. et al., 2006, preprint (astro-ph/0603451)
Hoekstra H., Yee H. K. C., Gladders M. D., 2002, ApJ, 577, 595
Hu W., 2005, Phys. Rev. D, 71, 047301
Jarvis M., Jain B., Bernstein G., Dolney D., 2005, ApJ, 644, 71
Jassal H. K., Bagla J. S., Padmanabhan T., 2005, MNRAS, 356, L11
Jeffreys H., 1961, Theory of Probability. Oxford Univ. Press, Oxford
Kamenshchik A. Y., Moschella U., Pasquier V., 2001, Phys. Lett., B511, 265
Kass R. E., Raftery A. E., 1995, J. Am. Stat. Assn., 90, 773
Kirkman D., Tytler D., Suzuki N., O'Meara J. M., Lubin D., 2003, ApJS, 149, 1
Knop R. A. et al., 2003, ApJ, 598, 102
Lewis A., Bridle S., 2002, Phys. Rev. D, 66, 103511
Liddle A. R., 2004, MNRAS, 351, L49
Linder E. V., 2006, Phys. Rev. D, 73, 063010
Maartens R., Majerotto E., 2006, Phys. Rev. D, 74, 023004
Mather J. C., Fixsen D. J., Shafer R. A., Mosier C., Wilkinson D. T., 1999, ApJ, 512, 511
Mena O., Santiago J., Weller J., 2006, Phys. Rev. Lett., 96, 041103
Mukherjee S., Feigelson E. D., Jogesh Babu G., Murtagh F., Fraley C., Raftery A., 1998, ApJ, 508, 314
Navarro I., Van Acoleyen K., 2005, A&A, in press (astro-ph/0512109)
Nesseris S., Perivolaropoulos L., 2005, Phys. Rev. D, 72, 123519
Nojiri S., Odintsov S. D., 2006, preprint (hep-th/0601213)
Onemli V. K., Woodard R. P., 2004, Phys. Rev. D, 70, 107301
Perlmutter S. et al., 1999, ApJ, 517, 565
Rapetti D., Allen S. W., Weller J., 2005, MNRAS, 360, 555
Reiprich T. H., Böhringer H., 2002, ApJ, 567, 716
Riess A. G. et al., 1998, ApJ, 116, 1009
Riess A. G. et al., 2004, ApJ, 607, 665
Sahni V., Saini T. D., Starobinsky A. A., Alam U., 2003, JETP Lett., 77, 201
Schuecker P., Caldwell R. R., Bohringer H., Collins C. A., Guzzo L., 2003, A&A, 402, 53
Schwarz G., 1978, Ann. Stat., 6, 461
Scranton R. et al., 2003, preprint (astro-ph/0307335)
Seljak U. et al., 2005, Phys. Rev. D, 71, 103515
Shapiro C., Turner M. S., 2005, ApJ, 649, 563
Spergel D. N. et al., 2003, ApJS, 148, 175
Spergel D. N. et al., 2006, preprint (astro-ph/0603449)
Steinhardt P. J., Wang L.-M., Zlatev I., 1999, Phys. Rev. D, 59, 123504
Tegmark M. et al., 2004, Phys. Rev. D, 69, 103501
Upadhye A., Ishak M., Steinhardt P. J., 2005, Phys. Rev. D, 72, 063501
van Waerbeke L. et al., 2000, A&A, 358, 30
Van Waerbeke L., Mellier Y., Hoekstra H., 2005, A&A, 429, 75
Verde L. et al., 2003, ApJS, 148, 195
Viel M., Weller J., Haehnelt M., 2004, MNRAS, 355, L23
Vikman A., 2005, Phys. Rev. D, 71, 023515
Visser M., 2004, Class. Quant. Grav., 21, 2603
Voevodkin A., Vikhlinin A., 2004, ApJ, 601, 610
Vollick D. N., 2003, Phys. Rev. D, 68, 063510
Weller J., Lewis A. M., 2003, MNRAS, 346, 987
Zhao G.-B., Xia J.-Q., Li M., Feng B., Zhang X., 2005, Phys. Rev. D, 72, 123515
Zhao G.-B., Xia J.-Q., Feng B., Zhang X., 2006, preprint (astro-ph/0603621)
Zlatev I., Wang L.-M., Steinhardt P. J., 1999, Phys. Rev. Lett., 82, 896

This paper has been typeset from a TEX/LATEX file prepared by the author.